

Cite this: DOI: 10.1039/c0xx00000x

www.rsc.org/dalton

PAPER

Remarkable enhancement of catalytic activity of a 2:1 complex between a non-planar Mo(V)-porphyrin and a ruthenium-substituted Keggin-type heteropolyoxometalate in catalytic oxidation of benzyl alcohols

Atsutoshi Yokoyama,^{a,b} Kei Ohkubo,^a Tomoya Ishizuka,^c Takahiko Kojima,^{*c} and Shunichi Fukuzumi^{*a,b}

Received (in XXX, XXX) Xth XXXXXXXXXX 20XX, Accepted Xth XXXXXXXXXX 20XX

DOI: 10.1039/b000000x

A 2:1 complex composed between a non-planar Mo(V)-porphyrin complex ($[\text{Mo}(\text{DPP})(\text{O})]^{+}$, DPP²⁻ = dodecaphenylporphyrin) and a ruthenium-substituted Keggin-type heteropolyoxometalate (Ru-POM), $[\text{SiW}_{11}\text{O}_{39}\text{Ru}^{\text{III}}(\text{DMSO})]^{5-}$, acts as an efficient catalyst for oxidation of benzyl alcohols with iodosobenzene as an oxidant in CDCl_3 at room temperature. The catalytic oxidation afforded the corresponding benzaldehydes, whereas neither the ammonium salt of Ru-POM nor $[\text{Mo}(\text{DPP})(\text{O})]^{+}$ alone exhibited catalytic reactivity under the same experimental conditions. This enhancement can be attributed to a large anodic shift of the redox potential of the ruthenium centre due to the complexation of the Ru-POM with two cationic $\{\text{Mo}(\text{DPP})(\text{O})\}^{+}$ units. The kinetic analysis demonstrated that the catalytic oxidation proceeded *via* formation of a catalyst-substrate complex, and electron-withdrawing substituents at the *para* position of benzyl alcohol accelerated the reaction. The rate constants of the oxidation reactions correlate to the bond dissociation energies of the C-H bonds of the substrate. A linear correlation was observed for logarithm of the rate constants of oxidation reactions of benzyl alcohols with that of hydrogen abstraction by cumyl peroxy radical, indicating the reaction proceeds *via* hydrogen abstraction. The observed kinetic isotope effect (KIE) indicates that the hydrogen abstraction occurs from the benzyl group rather than the hydroxy group.

Introduction

Polyoxometalates and heteropolyoxometalates (POMs) are widely known as functional materials in catalytic oxidation reactions,¹⁻¹⁴ photocatalytic reactions,^{15,16} medicines,¹⁷ and solid-state chemistry¹⁸ due to their robust structures and rich redox chemistry.¹⁹ Especially, a number of POMs and their derivatives were prepared as oxidation catalysts for the organic substrates, such as lacunary-type POM,⁷ “sandwich” type POM,⁸ and metallorganic-POM hybrid catalysts.⁹ In particular, the facile incorporation of transition-metals into lacunary-type POMs has attracted significant interest for preparation of oxidation catalysts with high activity.¹⁰ For example, a ruthenium-substituted Keggin-type POM (Ru-POM), $[\text{XW}_{11}\text{O}_{39}\text{Ru}^{\text{III}}(\text{H}_2\text{O})]^{5-}$ (X = P or Si, Fig. 1), catalyzes oxygenation reactions of hydrocarbons with various oxidants to afford the corresponding alcohols, aldehydes and carboxylic acids at relatively high temperature (> 60 °C).¹¹ Moreover, the Ru-POM can act as a heterogeneous catalyst for oxidations of alkanes and alcohols by using molecular oxygen as an oxidant.¹² In most cases, POMs are synthesized as inorganic salts (Na^{+} , K^{+} , and Cs^{+}), because they are only soluble in water and used with phase transfer catalysts under two-phase reaction conditions for organic substrates. In order to improve the solubility in organic solvents, many POMs have been prepared as

ammonium-salts ($[(\text{C}_4\text{H}_9)_4\text{N}]^{+}$ (TBA), $[(\text{C}_6\text{H}_{13})_4\text{N}]^{+}$ (THA)). However, the counter cation has yet to be utilized to improve the catalytic reactivity of POMs.

In this context, we have previously reported construction of 2:1 complexes composed of a non-planar Mo(V)-porphyrin, $[\text{Mo}(\text{DPP})(\text{O})(\text{H}_2\text{O})]^{+}$ (**1**) (DPP²⁻: dodecaphenylporphyrin, Figure 1), and Keggin-type POMs, which are soluble in toluene, chloroform (CHCl_3) and dichloromethane (CH_2Cl_2).²⁰ Each

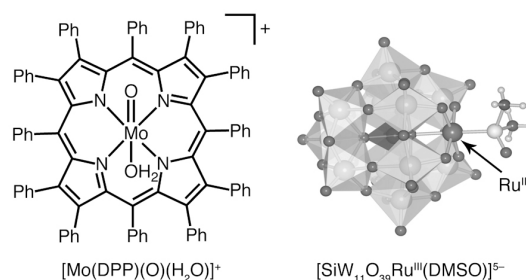


Fig. 1 Non-planar Mo(V)-porphyrin complex, $[\text{Mo}(\text{DPP})(\text{O})(\text{H}_2\text{O})]^{+}$ (**1**), and ruthenium-substituted Keggin-type POM, $[\text{SiW}_{11}\text{O}_{39}\text{Ru}^{\text{III}}(\text{DMSO})]^{5-}$ (**2**), used in this study.

component is connected *via* direct coordination bonds due to the high Lewis acidity of the Mo(V) center bound to the distorted porphyrin ligand and the strong coordination bonds make it

possible to maintain their structures in solution.²⁰ The merit of such complexes is not only the improvement of the solubility of

POMs into less polar solvents, but also the elevation of the oxidation potentials of POMs by coordination of the cationic metalloporphyrin unit. Thus, when metal-substituted POMs are employed in the metalloporphyrin-POM assembly, the oxidation potential of the inserted metal center is expected to be positively shifted to provide the higher reactivity in oxidation reactions. However, the catalytic reactivity of such a metalloporphyrin-POM assembly has yet to be examined.

We report herein formation of a 2:1 complex between a non-planar Mo(V)-porphyrin, ([Mo(DPP)(O)(H₂O)]⁺ (**1**)) and a Ru-POM ([SiW₁₁O₃₉Ru^{III}(DMSO)]⁵⁻ (**2**)) which acts an efficient catalyst for oxidation of benzyl alcohols^{13,14} by iodobenzene (PhIO) in CDCl₃ at room temperature to afford the corresponding benzaldehydes. The [Mo(DPP)(O)(H₂O)]⁺ unit is shown to play an essential role to enhance the catalytic reactivity of Ru-POM. The catalytic mechanism is clarified by the detailed kinetic study in comparison with the reactivity of cumyl peroxy radical in hydrogen abstraction from benzyl alcohols.

Experimental

Materials and methods

All chemicals available were purchased from appropriate commercial sources and used as received without further purification unless otherwise noted. Dichloromethane (CH₂Cl₂) and acetonitrile (CH₃CN) was distilled from CaH₂ under N₂ just prior to use. All other solvents were special grade and were used as received from commercial sources without further purification. Column chromatography was performed on a silica gel Waco-gel C-200 (60–200 mesh) or activated alumina (ca. 200 mesh), both from Waco Pure Chemicals. UV-vis spectroscopy was carried out on a JASCO V-570 UV/VIS/NIR spectrometer at room temperature. MALDI-TOF-MS spectra were recorded on a Bruker Daltonics ultrafleXtreme spectrometer using α -cyano-4-hydroxycinnamic acid (CHCA) as a matrix. EPR spectra were recorded on a Bruker EMXPlus 9.5/2.7 spectrometer in distilled and deaerated CH₂Cl₂ at 5 K.

Safety Note. *Caution!*

Perchlorate salts of metal complexes with organic ligands are potentially explosive. They should be handled with great care in small quantities.

Synthesis

[Mo(DPP)(O)(H₂O)]ClO₄ (**1**),²⁰ α -Cs_{4.9}K_{0.1}[SiW₁₁O₃₉Ru^{III}(DMSO)]^{11e}, deuterated benzyl alcohols (PhCH₂OD²¹ and PhCD₂OH²²) were prepared in accordance with the literature methods.

(TBA)₅[SiW₁₁O₃₉Ru^{III}(DMSO)]•3H₂O (**2**)

α -Cs_{4.9}K_{0.1}[SiW₁₁O₃₉Ru^{III}(DMSO)] (200 mg, 57 μ mol) and [(*n*-butyl)₄N]Br (TBABr) (193 mg, 600 μ mol) were dissolved in 20 mL of water and stirred vigorously at 50 °C for 3 hours. Dark orange precipitate was collected and wash by a large amount of water. Recrystallization from CH₃CN/H₂O gave dark orange powder, and was filtered and dried up under vacuum (115 mg, 49%). Anal. Calcd for C₈₂H₁₈₆N₅O₄₀SiW₁₁SRu•3H₂O: C 23.90, H

4.69, N 1.70. Found: C 23.63, H 4.20, N 1.63. IR spectrum (in KBr): $\nu_{S=O}$ 1100 cm⁻¹.

(TBA)₃{(Mo(DPP)(O))₂[SiW₁₁O₃₉Ru^{III}(DMSO)]} (**3**)

1 (100 mg, 69 μ mol) in 10 mL of CH₂Cl₂ was mixed with **2** (122 mg, 30 μ mol) dissolved in 10 mL of CH₃CN. The solution was heated at 50 °C for 3 hours and evaporated to dryness. Recrystallization from CH₂Cl₂/hexane gave dark greenish brown powder. The powder was dried up under vacuum (153 mg). MALDI-TOF-MS (negative mode): 5444.71 (observed, [M-DMSO + 2H]⁻); 5444.30 (calcd for [C₁₈₄H₁₂₂N₈O₄₁SiMo₂W₁₁]⁻). IR spectrum (in KBr): $\nu_{S=O}$ 1100 cm⁻¹. Anal. Calcd for **3**•1.5C₆H₁₄•10H₂O (C₂₄₃H₂₇₅N₁₁O₅₂SSiRuMo₂W₁₁): C, 44.51; H, 4.23; N, 2.35%. Found: C, 44.33; H, 4.50; N, 2.57%.

Electrochemical Measurements

Cyclic voltammograms (CV), differential pulse voltammograms (DPV) and second-harmonic AC voltammograms (SHACV) were obtained on an ALS 630B electrochemical analyzer in deaerated PhCN in the presence of 0.1 M [(*n*-butyl)₄N]PF₆ (TBAPF₆) as a supporting electrolyte under Ar at room temperature, with use of a glassy carbon electrode as a working electrode, Ag/AgNO₃ as a reference electrode, a Pt wire as a auxiliary electrode. All potentials were calibrated with respect to the ferrocene/ferrocenium redox couple as 0 V.

General Procedure for Oxidation of Alcohols and Aldehydes

Reactions were carried out in a light-shielded glass vial (5 mL). 100 μ mol of the each substrate (*p*-nitro-, *p*-chloro-, *o*-chloro-, *p*-methyl- and *o*-methylbenzyl alcohols, benzyl alcohol, *p*-nitro- and *p*-methoxybenzaldehyde), iodobenzene (44 mg, 200 μ mol) and 1 μ mol of the each catalyst (**1**, **2**, and **3**) were dissolved in 600 μ L of CDCl₃ at room temperature. Monitoring reactions were performed by ¹H NMR measurements; 50 μ L of each reaction mixture was filtered and diluted by 500 μ L of CDCl₃.

Results and discussion

Preparation of a Mo(V)-porphyrin-[Ru-POM] assembly

A non-planar Mo(V)-porphyrin ([Mo(DPP)(O)(H₂O)]ClO₄ (**1**)²⁰) and a Ru-POM, (TBA)₅[SiW₁₁O₃₉Ru^{III}(DMSO)] (**2**)^{11e}, were used in this study (Fig. 1). The reaction of **1** and **2** was carried out in a mixed solvent (CH₂Cl₂/CH₃CN) at 50 °C to obtain the mixed complex, [{Mo(DPP)(O)}₂(H₂SiW₁₁O₃₉Ru(DMSO))] (3). The coordination of DMSO was confirmed by IR spectroscopy to observe $\nu_{S=O}$ at 1100 cm⁻¹, which was consistent with that observed for **2**. After removing the solvents, crystallization from CH₂Cl₂/hexane gave dark greenish brown powder. In the MALDI-TOF-MS spectrum of **3**, a molecular ion peak cluster was observed at 5444.71 (*m/z*) with use of CHCA (α -cyano-4-hydroxycinnamic acid) as a matrix (Fig. 2), assignable to that of a diprotonated 2:1 assembly of [Mo(DPP)(O)]⁺ unit and [SiW₁₁O₃₉Ru^{III}]⁵⁻ ([{Mo(DPP)(O)}₂(H₂SiW₁₁O₃₉Ru^{III})]⁻ (**3** - DMSO)⁻): *m/z* = 5444.30). This result indicates that the POM coordinates to the Mo(V) center directly in place of the H₂O ligand. On the basis of crystal structures of hybrid complexes composed of two {Mo^V(DPP)(O)} fragments and one Keggin-type POM,¹⁹ the Mo^V(DPP)(O) moiety in **3** should form a coordination bond with one of the terminal oxo ligands of the

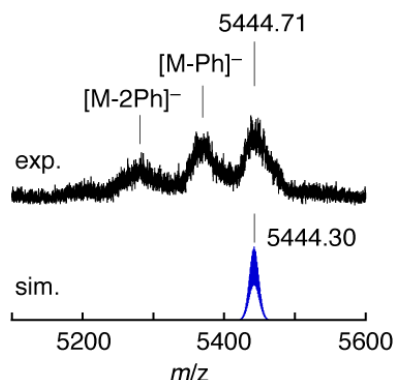


Fig. 2 MALDI-TOF-MS spectrum of a 2:1 assembly made of **1** and **2** ($m/z = 5444.71$) in CH_2Cl_2 (linear negative mode, matrix; α -cyano-4-hydroxycinnamic acid (CHCA)) and its computer simulation ($[\{\text{Mo}(\text{DPP})(\text{O})\}_2(\text{H}_2\text{SiW}_{11}\text{O}_{39}\text{Ru}^{\text{III}})]^-$; $m/z = 5444.30$).

Ru^{III} -substituted Keggin-type polyoxometalate.

Oxidation states of molybdenum and ruthenium in **3**

In the EPR spectrum of **2**, a signal assigned to Ru^{III} ($S = 1/2$) was observed at $g_x = 2.289$, $g_y = 2.209$, and $g_z = 1.873$ in CH_2Cl_2 at 5 K (Fig. 3a).^{11b,23} As for **3**, two kinds of signals were observed;

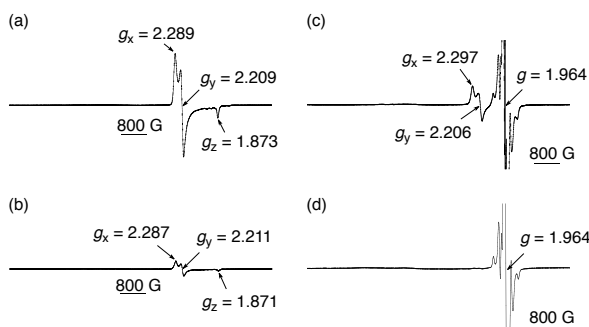


Fig. 3 EPR spectra of (a) **2** (0.2 mM), (b) **2** (0.2 mM) and PhIO (40 mM), (c) **3** (0.2 mM) and (d) **3** (0.2 mM) and PhIO (40 mM) for the Mo^{V} ($S = 1/2$, $I = 0$) and Ru^{III} ($S = 1/2$) at 5 K in CH_2Cl_2 : Frequency, 9.39 GHz; Power, 10 mW; Modulation; 100 GHz, 10 G.

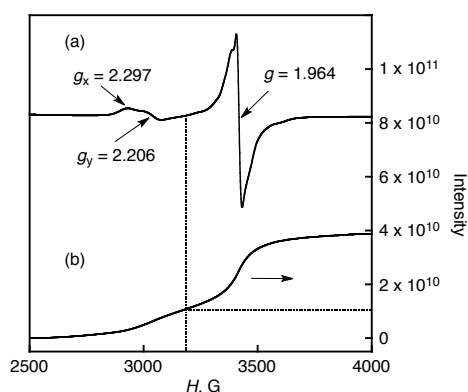


Fig. 4 (a) EPR spectrum of **2** and (b) its double-integral spectrum for the Mo^{V} ($S = 1/2$, $I = 0$) and Ru^{III} ($S = 1/2$) at 5 K in CH_2Cl_2 : Frequency, 9.39 GHz; Power, 1 mW; Modulation; 100 GHz, 10 G. Spectra of Mo^{V} and Ru^{III} are overlapped at 3300 G, and g_z of Ru^{III} is totally overlapped with Mo^{V} . Dashed line shows a round boundary of Ru^{III} and Mo^{V} .

one at $g = 1.964$ was assigned to that of the Mo^{V} center ($S = 1/2$, $I = 0$),²⁰ and the other signal at $g_x = 2.297$ and $g_y = 2.206$ was assigned to that of the Ru^{III} ($S = 1/2$) center (the g_z signal of the Ru^{III} center in **3** was overlapped with that of Mo^{V} , Figure 3c). This result indicates that the ruthenium ions in **2** and **3** are intact to be in the Ru^{III} oxidation state. The double-integration of the EPR signal due to **3** indicates that the ratio of Mn^{V} to Ru^{III} is 2:1, reflecting the MALDI-TOF-MS spectrum (Fig. 4).

When PhIO was added to the **2** and **3**, the signals assigned to Ru^{III} centers diminished for **2** or completely disappeared for **3** as depicted in Fig. 3b and 3d, respectively. This result indicates that EPR-silent ruthenium species may be $\text{Ru}(\text{IV})$ -oxo complexes to act as reactive intermediates in catalytic oxidation of organic substrates (*vide infra*).

Electrochemical measurements

Electrochemical measurements of **1**, **2** and **3** were carried out in CH_2Cl_2 in the presence of 0.1 M TBAPF₆ as an electrolyte under Ar (Fig. 5 and Table 1) at room temperature. As for **1**, reduction and oxidation waves of the porphyrin unit were observed at -1.57 V ($\text{Por}^{3-}/\text{Por}^{2-}$), 0.76 V ($\text{Por}^{2-}/\text{Por}^-$), and 1.12 V ($\text{Por}^-/\text{Por}^0$), respectively.²⁴ The redox wave at -0.46 V was assigned to reduction of $\text{Mo}(\text{V})$ ion ($\text{Mo}^{\text{IV}}/\text{Mo}^{\text{V}}$). Based on the EPR measurement, the first and second oxidation redox waves of **2** are assigned to $\text{Ru}^{\text{III}}/\text{Ru}^{\text{IV}}$ (0.07 V) and $\text{Ru}^{\text{IV}}/\text{Ru}^{\text{V}}$ (0.86 V), respectively. In the case of **3**, and irreversible redox wave was observed below -1.0 V. According to the DPV measurement of **3**, the one- and two-electron oxidation processes of the ruthenium center ($\text{Ru}^{\text{III}}/\text{Ru}^{\text{IV}}$ and $\text{Ru}^{\text{IV}}/\text{Ru}^{\text{V}}$) were observed at 0.90 V and 1.28 V, whereas the one- and two-electron oxidation processes of the porphyrin unit ($\text{Por}^{2-}/\text{Por}^-$ and $\text{Por}^-/\text{Por}^0$) at 0.73 V and 1.15 V, respectively. Thus, the large anodic shifts of the redox potentials of the ruthenium center in **3** were observed, resulting from the strong coordination of the cationic $[\text{Mo}(\text{DPP})(\text{O})]^+$ unit to the POM unit.

Catalytic oxidation reactions of benzyl alcohols

With use of **3**, catalytic oxidation reactions of benzyl alcohol (*p*-H) and its *para*-substituted and *ortho*-substituted derivatives with PhIO were carried out in CDCl_3 at room temperature (Scheme 1). The reactions ($[\text{substrate}] = 160$ mM, $[\text{oxidant}] = 330$ mM, $[\text{catalyst}] = 1.6$ mM) were performed in the light shielded vials and the conversions were monitored by ^1H NMR measurements. As comparison, the reactivity of precursors (**1** and **2**) was also examined as homogeneous catalysts for each reaction.

The ^1H NMR spectra after the reactions for 6 hours were shown in Fig. 6. The oxidation reaction can be stopped by

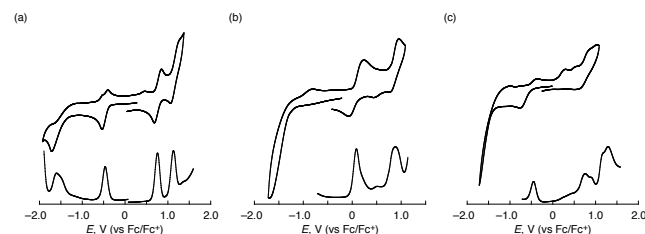


Fig. 5 Cyclic voltammograms (CV) and differential pulse voltammograms (DPV) of (a) **1**, (b) **2** and (c) **3** in CH_2Cl_2 at room temperature under Ar in the presence of 0.1 M TBAPF₆.

Table 1 Redox potentials of **1**, **2** and **3** in CH₂Cl₂.^a

compound	<i>E</i> vs. Fc/Fc ⁺ , V						POM ⁹⁻ /POM ⁸⁻ ^c
	Mo ^{IV} /Mo ^V	Por ²⁻ /Por ^{-b}	Por ⁻ /Por ⁰	Por ³⁻ /Por ²⁻	Ru ^{III} /Ru ^{IV}	Ru ^{IV} /Ru ^V	
1	-0.46	0.76	1.12	-1.57	–	–	–
2	–	–	–	–	0.07	0.86	irreversible
3	-0.44	0.73	1.15	irreversible	0.90	1.28	irreversible

^a At room temperature under Ar; 0.1 M TBAPF₆ as an electrolyte. ^b Porⁿ⁻: DPP²⁻ ligand. ^c POMⁿ⁻: lacunary Keggin-type heteropolyoxometalate

Scheme 1

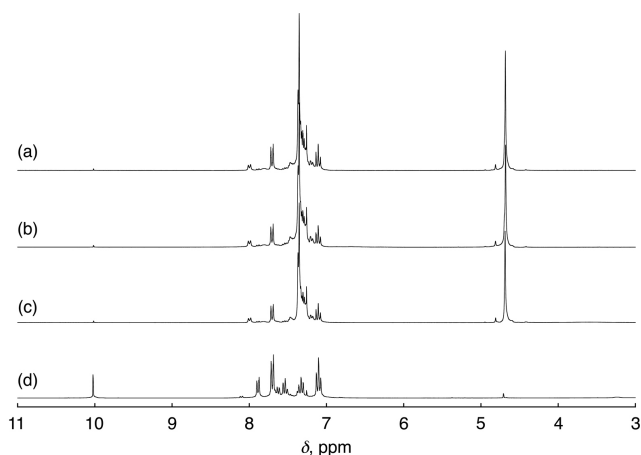
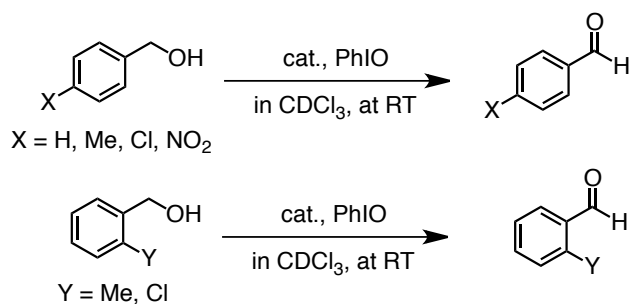


Fig. 6 ¹H NMR spectra of the reaction mixtures of benzyl alcohol after 60 h in CDCl₃ ([sub] = 160 mM, [PhIO] = 330 mM, [cat] = 1.6 mM). Each fraction contains (a) no catalyst, (b) complex **1**, (c) complex **2**, and (d) assembly **3** as a catalyst, respectively.

5 filtering the reaction mixture to eliminate the insoluble oxidant. This manipulation allows us to follow the reaction by ¹H NMR measurements. In the case of benzyl alcohol (*p*-**H**) as a substrate in the absence of catalyst, only the substrate and iodobenzene (PhI) derived from the decomposition of PhIO were detected by NMR measurements (Fig. 6a). When the complex **1** and **2** were used as catalysts, the catalytic oxidation hardly occurred at room temperature as compared to the blank reaction (Figs. 6b, c). In sharp contrast, the addition of **3** efficiently afforded benzaldehyde as an oxidation product from *p*-**H** (Fig. 6d). Obviously, this result indicates that coordination of the [Mo(DPP)(O)]⁺ unit to the Ru-POM significantly enhanced its reactivity as a oxidation catalyst probably due to the large anodic shift of redox potentials of ruthenium ion in complex **3** (vide supra). MALDI-TOF-MS measurement suggested that **3** could maintain the structure after the oxidation of *p*-**H** in CDCl₃ (see Fig. S1 in ESI).

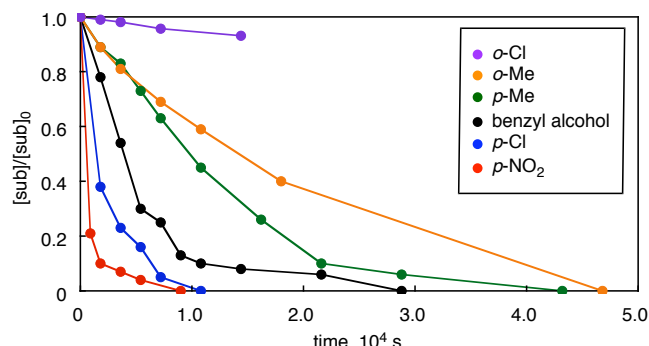


Fig. 7 Time profiles of consumption ($[sub]/[sub]_0$) of benzyl alcohols (substrates) in CDCl₃ at room temperature with use of TMS (tetramethylsilane) as an internal standard ($[sub]_0 = 160$ mM, [PhIO] = 330 mM, [**3**] = 1.6 mM, [TMS] = 16 mM). The consumption of each substrate was determined on the basis of the peak integration ratio for benzyl alcohols and TMS in ¹H NMR spectra.

Next, benzyl alcohol derivatives (*p*-nitrobenzyl alcohol (*p*-NO₂), *p*(*o*)-chlorobenzyl alcohol (*p*(*o*)-Cl) and *p*(*o*)-methylbenzyl alcohol (*p*(*o*)-Me)) were employed as substrates and the conversions from benzyl alcohols to the corresponding benzaldehydes at 60 min are summarized in Table 2.²⁵ The conversion was determined by the integration ratio of the peaks due to the substrates and the products in ¹H NMR spectra. The results in Table 2 clearly indicate that the catalytic oxidation reaction showed a significant substituent effect: the electron-withdrawing group accelerates the oxidation reaction while the electron-donating group slows down the reaction. Additionally, when the chloro or the methyl groups was introduced at the *ortho*-position of *p*-**H**, remarkable retardation of the substrate consumption was observed (Fig. 7), suggesting the existence of strong steric effect of the *o*-substituents.

Plots of $-\ln[sub]$ vs. time for oxidation of *p*-**H**, *p*-NO₂, *p*-Cl and *p*-Me by **3** as a catalyst were made as depicted in Fig. 8 to determine the pseudo-first-order rate constants (k_{obs}). The k_{obs} values thus determined are also summarized in Table 2. The one-electron oxidation potentials (E_{ox}) of benzyl alcohols were determined by second harmonic AC voltammetry (SHACV) in CH₂Cl₂ as summarized in Table 2. As expected, *p*-NO₂ showed

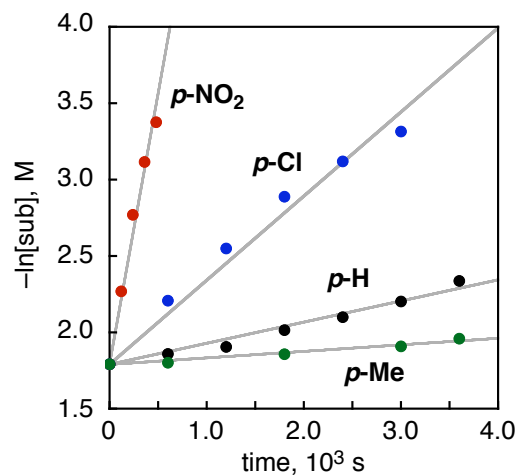


Fig. 8 Plots of $-\ln[\text{sub}]$ vs. time for catalytic oxidation of *p*-H (black), *p*-NO₂ (red), *p*-Cl (blue), and *p*-Me (green) by **3** with use of PhIO.

Table 2 Summary of conversions (%) and pseudo-first-order rate constants (s⁻¹) of the catalytic oxidation reactions in CDCl₃, and oxidation potentials (E_{ox}) of benzyl alcohols in CH₂Cl₂

substrate	conversion (%) ^a	k_{obs} (s ⁻¹)	E_{ox} ^b vs. Fc/Fc ⁺ , V
<i>p</i> -H ^c	41	1.4×10^{-4}	1.48
<i>p</i> -NO ₂	93	3.5×10^{-3}	1.72
<i>p</i> -Cl	77	5.5×10^{-4}	1.54
<i>o</i> -Cl	2	–	–
<i>p</i> -Me	19	4.3×10^{-5}	1.38
<i>o</i> -Me	17	–	–

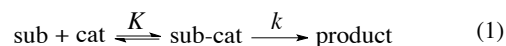
^aConversions were determined by ¹H NMR spectra in CDCl₃ at 60 min.

^bThe oxidation potentials (E_{ox}) of benzyl alcohols were determined by SHACV in CH₂Cl₂ in the presence of TBAPF₆ as a supporting electrolyte under Ar at room temperature. ^c*p*-H: benzyl alcohol

the highest oxidation potential because of the electron-withdrawing NO₂ group, whereas *p*-Me exhibited the lowest oxidation potential due to the electron-donating Me group. Because the higher the oxidation potential, the higher is the reactivity (Table 2), electron transfer (ET) from the substrate to the catalyst cannot be involved as the rate-determining step of the catalytic reaction. Electron donating substituents stabilize a positively charged transition state (e.g., in hydride transfer), whereas electron withdrawing substituents stabilize a negatively charged transition state (e.g., in proton transfer).^{14,26-28} Thus, the increase in the rate constant of the catalytic oxidation of benzyl alcohol derivatives with **3** with increasing the oxidation potentials of benzyl alcohols in Table 2 suggests the formation of a negatively charged transition state rather than a positively charged transition state. Such a substituent effect has often been observed in the catalytic oxidation of *para*-substituted benzyl alcohol derivatives.^{14,28} Because the acidity of the benzylic hydrogen increases with increasing the oxidation potentials of

benzyl alcohols, the acidity of the benzylic hydrogen may be involved in determining the catalytic reactivity presented in Table 2 as discussed below. In addition, a Hammett plot was made for the rate constants listed in Table 2 (see Fig. S2 in ESI). The ρ value was determined to be 1.91 ± 0.31 , also indicating that the proton transfer from the benzylic C-H bond to the reactive species should be important in the catalytic oxidation of benzyl alcohol derivatives with **3** and PhIO (*vide infra*).

As for *p*-H and *p*-NO₂, the concentration dependence of k_{obs} was examined as shown in Fig. 9. As a result, the saturation behaviors of k_{obs} at higher concentration of the substrates were observed in both cases. This result indicates that there is a pre-equilibrium to form an adduct between substrate and the catalyst prior to the oxidation reaction. In light of a discussion on the location of the proton in a Keggin-type POM (H₃[PW₁₂O₄₀]•6H₂O),²⁹⁻³² the substrate may bind to μ -oxo bridge neighboring active species (Ru(IV)=O) *via* hydrogen bond due to the stronger basicity of the μ -oxo bridge. The first-order rate constant (k) and binding constant (K) were determined by curve fitting to be $k = (2.3 \pm 0.8) \times 10^{-4} \text{ s}^{-1}$, $K = 10 \pm 2 \text{ M}^{-1}$ for *p*-H and $k = (4.4 \pm 0.3) \times 10^{-3} \text{ s}^{-1}$, $K = 21 \pm 6 \text{ M}^{-1}$ for *p*-NO₂ based on the following equations:



$$k_{\text{obs}} = \frac{kK[\text{substrate}]}{1 + K[\text{substrate}]} \quad (2)$$

where K is a binding constant, k is a first-order rate constant, $[\text{substrate}]$ is substrate concentration. Thus, *p*-NO₂ exhibited a larger binding constant reflecting the smaller $\text{p}K_{\text{a}}$ value compared with *p*-H.³²

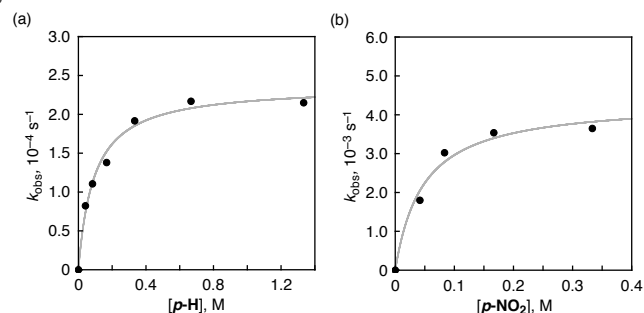


Fig. 9 Dependence of k_{obs} on concentrations (a) benzyl alcohol (*p*-H) and (b) *p*-nitrobenzyl alcohol (*p*-NO₂) for the oxidation with **3** in CDCl₃, and curve fitting (solid line) with use of eqn (2).

Mechanistic insights into the oxidation reaction

To gain further mechanistic insights into the catalytic oxidation of benzyl alcohol, two kinds of deuterated benzyl alcohols were employed to determine the kinetic isotope effects (KIE, $k_{\text{H}}/k_{\text{D}}$), PhCH₂OD²¹ and PhCD₂OH.²² The oxidation reaction of PhCD₂OH (1.6 mM) was performed in CHCl₃ in the presence of CDCl₃ (1.6 mM) and CD₃CN (1.6 mM) as internal standards. The time course of the reaction was monitored by ²H NMR spectroscopy. As shown in Fig. 10, the KIE value for PhCH₂OD was determined to be $k_{\text{H}}/k_{\text{D}} = 1.0$, and that for PhCD₂OH was

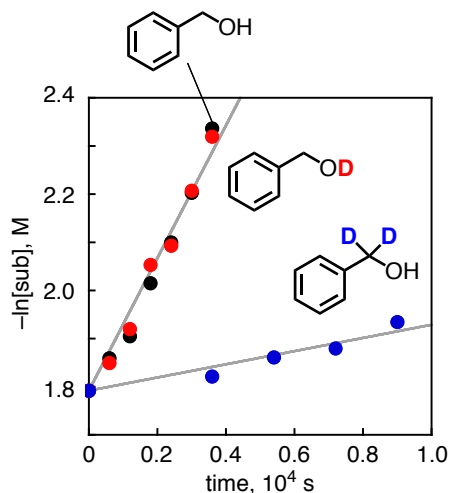


Fig. 10 Plots of $-\ln[\text{sub}]$ vs. time for the oxidation reactions of PhCH₂OH (black), PhCH₂OD (red) and PhCD₂OH (blue) by PhIO in the presence of **3** in CDCl₃ at room temperature (293 K).

determined to be $k_{\text{H}}/k_{\text{D}} = 10.14$. This indicates that the hydrogen abstraction occurs from the benzyl position of benzyl alcohol rather than the hydroxy position.

Based on the results described above, the catalytic oxidation reaction may proceed as follows: (1) A reactive species, presumably a Ru^{IV}=O species, is formed by the reaction of **3** with PhIO.³⁴ (2) The substrate binds to a μ -oxo bridge neighboring the Ru^{IV}=O moiety by using hydrogen bonding. (3) Hydrogen abstraction occurs at the benzyl position by the Ru^{IV}=O species.

In order to compare the observed substituent effect on the catalytic oxidation of benzyl alcohol derivatives in Table 2 with that on the authentic hydrogen abstraction reaction from benzyl alcohol derivatives, we examined the hydrogen abstraction of benzyl alcohol derivatives by cumyl peroxy radical (CumOO[•]). CumOO[•] was generated by photoirradiation in the oxygen-saturated CH₂Cl₂ solution containing di-*tert*-butyl peroxide (1.0 M) and cumene (1.0 M) at 183 K.³⁵ The decay of the EPR signal at $g = 2.016$ due to CumOO[•] in the presence of benzyl alcohols was monitored (Fig. 11) to determine the rate constants of hydrogen abstraction from benzyl alcohols by CumOO[•]. The second-order rate constants were determined to be $k = 7.2 \times 10^{-2}$

Table 3 Second-order rate constants for hydrogen abstraction from benzyl alcohols by cumyl peroxy radical in CH₂Cl₂ at -90 °C.

substrate	$k, \text{M}^{-1} \text{s}^{-1}$
<i>p</i> -NO ₂	1.4
<i>p</i> -Cl	8.4×10^{-1}
<i>p</i> -H	1.8×10^{-1}
<i>p</i> -Me	7.2×10^{-2}
<i>p</i> -OMe	2.6×10^{-2}
<i>o</i> -Me	$< 1 \times 10^{-2}$
<i>o</i> -Cl	$< 1 \times 10^{-2}$

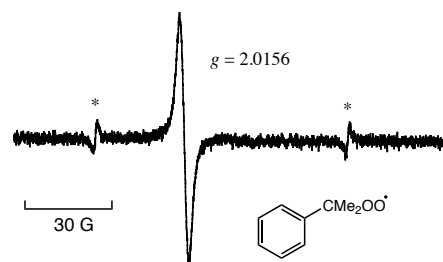


Fig. 11 EPR spectrum of cumyl peroxy radical in CH₂Cl₂ at 183 K generated in the photoirradiation of an oxygen-saturated CH₂Cl₂ solution containing di-*tert*-butyl peroxide (1.0 M) and cumene (1.0 M). The asterisk (*) denotes the Mn^{II} marker.

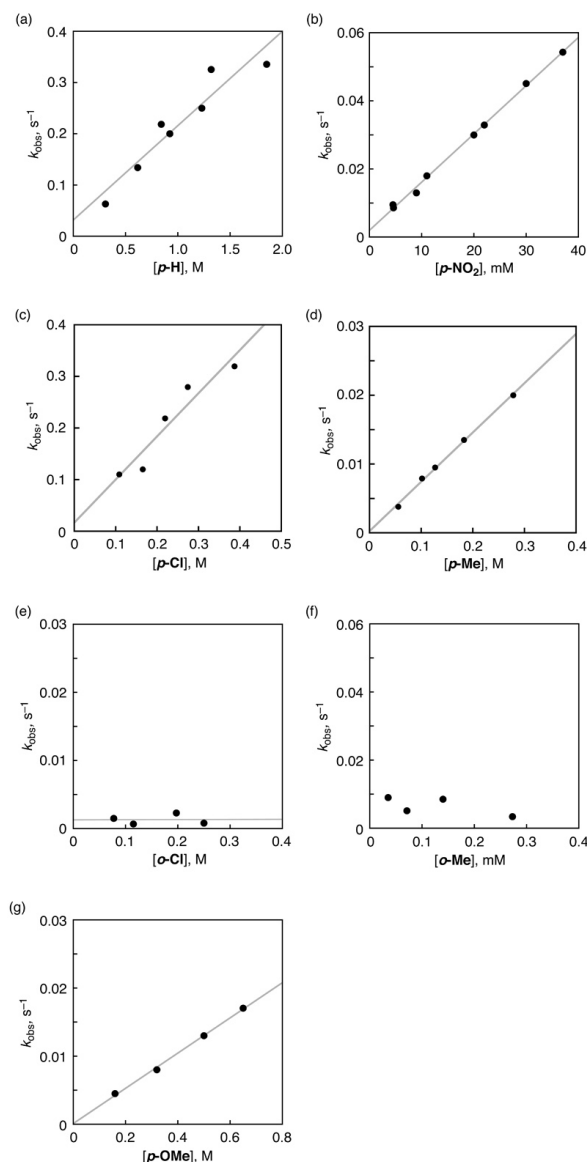


Fig. 12 Dependence of k_{obs} for hydrogen atom abstraction reaction of (a) benzyl alcohol (*p*-H), (b) *p*-nitrobenzyl alcohol (*p*-NO₂), (c) *p*-chlorobenzyl alcohol (*p*-Cl), (d) *p*-methylbenzyl alcohol (*p*-Me), (e) *o*-chlorobenzyl alcohol (*o*-Cl), (f) *o*-methylbenzyl alcohol (*o*-Me) and (g) *p*-methoxybenzyl alcohol (*p*-OMe) by cumyl peroxy radical on concentrations of benzyl alcohols in CH₂Cl₂ at 183 K.

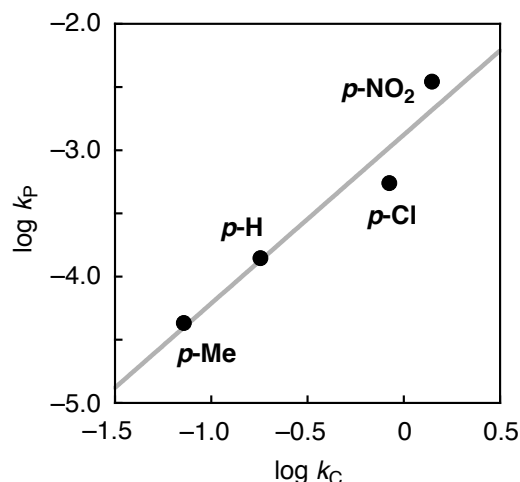


Fig. 13 Plot of logarithm of the pseudo-first order rate constants of the catalytic oxidation of benzyl alcohols with **3** (k_p) at room temperature vs. logarithm of the second-order rate constants of hydrogen abstraction from benzyl alcohols by CumOO \cdot (k_c) at 183 K. The k_p values were determined by ^1H NMR in CDCl_3 ([substrate] = 160 mM, [oxidant] = 330 mM, [catalyst] = 1.6 mM), and the k_c values were determined by the decay of EPR signal of CumOO \cdot in the presence of benzyl alcohols in CH_2Cl_2 .

10^{-1} s^{-1} for *p*-Me, $k = 0.2 \text{ M}^{-1} \text{ s}^{-1}$ for *p*-H and $k = 1.4 \text{ M}^{-1} \text{ s}^{-1}$ for *p*-NO $_2$ (Fig. 12 and Table 3). The order of the rate constants for hydrogen abstraction from benzyl alcohols was *p*-NO $_2$ > *p*-Cl > *p*-H > *p*-Me. This order agrees with that of activation energy (E_a) of H-abstraction reaction.³⁵ There is a good linear correlation between the logarithm of the catalytic rate constants (k_p) of oxidation of benzyl alcohols with **3** and that of the rate constants (k_c) of hydrogen abstraction from benzyl alcohols by cumyl peroxy radicals as shown in Fig. 13. Thus, the substituent effect on the oxidation of benzyl alcohols with **3** results from that on the rate-determining hydrogen abstraction step from benzyl alcohols by the Ru^{IV}=O species.

Conclusions

A ruthenium-substituted metalloporphyrin-POM complex was prepared, acting as an efficient catalyst for oxidation of benzyl alcohols with PhIO as an oxidant in CDCl_3 at room temperature. The coordination of the cationic Mo(V)-porphyrin unit is effective not only for the improvement of solubility of POM toward low polar solvent, but also for remarkable enhancement of catalytic activity in the oxidation reactions. Benzyl alcohols were oxidized to corresponding benzaldehydes via the formation of a catalyst-substrate adduct probably through intermolecular hydrogen bonding. The hydrogen abstraction occurs at the benzyl position, exhibiting a large KIE. Our strategy will provide a new category of POM-based catalytic oxidation systems with high efficiency.

Acknowledgments

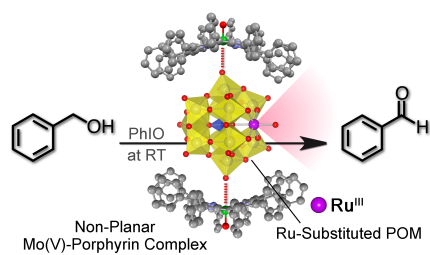
We are grateful to financial support provided by Grants-in-Aid (Nos. 20108010 and 21111501), a Global COE program, "the Global Education and Research Centre for Bio-Environmental Chemistry" from the Japan Society of Promotion of Science (JSPS), a JSPS predoctoral fellowship (20-00804 to A. Y.), Japan

and KOSEF/MEST through WCU project (R31-2008-10010-0), Korea.

Notes and references

- ^a Department of Material and Life Science, Graduate School of Engineering, Osaka University, ALCA, Japan Science and Technology Agency (JST), 2-1 Yamada-oka, Suita, Osaka 565-0871, Japan. E-mail: fukuzumi@chem.eng.osaka-u.ac.jp
- ^b Department of Bioinspired Chemistry (WCU), Ewha Womans University, Seoul 120-750, Korea
- ^c Department of Chemistry, Graduate School of Pure and Applied Science, University of Tsukuba, 1-1-1 Tennoudai, Tsukuba, Ibaraki 305-8571, Japan. E-mail: kojima@chem.tsukuba.ac.jp
- † Electronic Supplementary Information (ESI) available: MALDI-TOF-MS spectra. See DOI: 10.1039/b000000x/
- M. T. Pope, in *Heteropoly and Isopoly Oxometalates*, Springer-Verlag, Berlin, **1983**; C. L. Hill and C. M. Prosser-MacCartha, *Coord. Chem. Rev.*, **1995**, **143**, 407; I. V. Kozhevnikov, *Chem. Rev.*, **1998**, **98**, 171; N. Mizuno and M. Misono, *Chem. Rev.*, **1998**, **98**, 199; R. Neumann, *Prog. Inorg. Chem.*, **1998**, **47**, 317; A. Proust, R. Thouvenot and P. Gouzerh, *Chem. Commun.*, **2008**, 1837; N. Dupré, P. Rémy, K. Micoine, C. Boglio, S. Thorimbert, E. Lacôte, B. Hasenkopf and M. Malacria, *Chem.-Eur. J.*, **2010**, **16**, 7256; R. Ishimoto, K. Kamata and N. Mizuno, *Angew. Chem., Int. Ed.*, **2009**, **48**, 8900; A. M. Khenkin and R. Neumann, *J. Am. Chem. Soc.*, **2008**, **130**, 14474.
 - D. E. Katsoulis and M. T. Pope, *J. Am. Chem. Soc.*, **1984**, **106**, 2737; D. E. Katsoulis and M. T. Pope, *J. Chem. Soc., Chem. Commun.*, **1986**, 1186; D. E. Katsoulis and M. T. Pope, *J. Chem. Soc., Dalton Trans.*, **1989**, 1483; C. Rong and M. T. Pope, *J. Am. Chem. Soc.*, **1992**, **114**, 2932; A. Bagno, M. Bonchio, A. Sartorel and G. Scorrano, *Eur. J. Inorg. Chem.*, **2000**, 17.
 - Q. Yin, J. M. Tan, C. Besson, Y. V. Geletii, D. G. Musaev, A. E. Kuznetsov, Z. Luo, K. I. Hardcastle and C. L. Hill, *Science*, **2010**, **328**, 342; Y. V. Geletii, Z. Huang, Y. Hou, D. G. Musaev, T. Lian and C. L. Hill, *J. Am. Chem. Soc.*, **2009**, **131**, 7522; Y. V. Geletii, B. Botar, P. Kögerler, D. A. Hillesheim, D. G. Musaev and C. L. Hill, *Angew. Chem., Int. Ed.*, **2008**, **47**, 3896; A. Sartorel, M. Carraro, G. Scorrano, R. D. Zorzi, S. Geremia, N. D. McDaniel, S. Bernhard and M. Bonchio, *J. Am. Chem. Soc.*, **2008**, **130**, 5006.
 - R. Neumann, *Inorg. Chem.*, **2010**, **49**, 3594; R. Neumann and M. Dahan, *J. Am. Chem. Soc.*, **1998**, **120**, 11969.
 - K. Kamata, R. Ishimoto, T. Hirano, S. Kuzuya, K. Uehara and N. Mizuno, *Inorg. Chem.*, **2010**, **49**, 2471.
 - D.-L. Long, R. Tsunashima and L. Cronin, *Angew. Chem., Int. Ed.*, **2010**, **49**, 1736.
 - K. Kamata, K. Yonehara, Y. Sumida, K. Yamaguchi, S. Hikichi and N. Mizuno, *Science*, **2003**, **300**, 964; K. Kamata, Y. Nakagawa, K. Yamaguchi and N. Mizuno, *J. Catal.*, **2004**, **224**, 224; K. Kamata, M. Kotani, K. Yamaguchi, S. Hikichi and N. Mizuno, *Chem.-Eur. J.*, **2007**, **13**, 639; R. Prabhakar, K. Morokuma, C. L. Hill and D. G. Musaev, *Inorg. Chem.*, **2006**, **45**, 5703; A. Sartorel, M. Carraro, A. Bagno, G. Scorrano and M. Bonchio, *Angew. Chem., Int. Ed.*, **2007**, **46**, 325; M. Carraro, L. Sandei, A. Sartorel, G. Scorrano and M. Bonchio, *Org. Lett.*, **2006**, **8**, 3671; W. Zhao, Y. Zhang, B. Ma, Y. Ding and W. Qiu, *Catal. Commun.*, **2010**, **11**, 527.
 - Y. Kikukawa, K. Yamaguchi and N. Mizuno, *Inorg. Chem.*, **2010**, **49**, 8194; R. Neumann and A. M. Khenkin, *Inorg. Chem.*, **1995**, **34**, 5753; R. Neumann, A. M. Khenkin and M. Dahan, *Angew. Chem., Int. Ed.*, **1995**, **34**, 1587; R. Neumann and M. Dahan, *Nature*, **1997**, **388**, 353.
 - J. Ettetdgui and R. Neumann, *J. Am. Chem. Soc.*, **2009**, **131**, 4.
 - R. Neumann and M. Gara, *J. Am. Chem. Soc.*, **1995**, **117**, 5066; N. Mizuno, C. Nozaki, I. Kiyoto and M. Misono, *J. Am. Chem. Soc.*, **1998**, **120**, 9267; R. Neumann and M. Gara, *J. Am. Chem. Soc.*, **1955**, **117**, 5066; Y. Nakazawa, K. Kamata, M. Kotani, K. Yamaguchi and N. Mizuno, *Angew. Chem., Int. Ed.*, **2005**, **44**, 5136; J. Wang, L. Yan,

- G. Li, X. Wang, Y. Ding and J. Suo, *Tetrahedron Lett.*, 2005, **46**, 7023.
- 11 R. Neumann and C. Abu-Gnim, *J. Chem. Soc., Chem. Commun.*, 1989, 1324; R. Neumann and C. Abu-Gnim, *J. Am. Chem. Soc.*, 1990, **112**, 6025; K. Filipek, *Inorg. Chim. Acta*, 1995, **231**, 237; R. Neumann and M. Dahan, *Polyhedron*, 1998, **17**, 3557; M. Sadakane and M. Higashijima, *Dalton Trans.*, 2003, 659; M. Sadakane, D. Tsukuma, M. H. Dickman, B. Bassil, U. Kortz, M. Hagashijima and W. Ueda, *Dalton Trans.*, 2006, 4271.
- 10 12 R. Neumann, M. Dahan, *Polyhedron*, **1998**, *17*, 3557.; K. Yamaguchi and N. Mizuno, *New J. Chem.* **2002**, *26*, 972–974
- 13 R. Neumann and M. Levin, *J. Org. Chem.*, 1991, **56**, 5707; R. Neumann, A. M. Khenkin, D. Juwiler, H. Miller and M. Gara, *J. Mol. Catal. A: Chem.*, 1997, **117**, 169; R. Ben-Daniel, P. Alsters and R. Neumann, *J. Org. Chem.*, 2001, **66**, 8650; D. Sloboda-Rozner, P. L. Alsters and R. Neumann, *J. Am. Chem. Soc.*, 2003, **125**, 5280; V. N. Panchenko, I. Borbáth, M. N. Timofeeva and S. Göbbölös, *J. Mol. Catal. A: Chem.*, 2010, **319**, 119; A. Haimov and R. Neumann, *Chem. Commun.*, 2002, 876.
- 20 14 A. M. Khenkin and R. Neumann, *J. Org. Chem.*, 2002, **67**, 7075; A. M. Khenkin, L. J. W. Shimon and R. Neumann, *Inorg. Chem.*, 2003, **42**, 3331.
- 15 T. Yamase, *Chem. Rev.*, 1998, **98**, 307; A. Dolbecq, E. Dumas, C. R. Mayer and P. Mialane, *Chem. Rev.*, 2010, **110**, 6009.
- 25 16 J. Ettetdgui, Y. Diskin-Posner, L. Weiner and R. Neumann, *J. Am. Chem. Soc.*, 2011, **133**, 188.
- 17 J. T. Rhule, C. L. Hill and D. A. Judd, *Chem. Rev.*, 1998, **98**, 327.
- 18 O. Nakamura, T. Kodama, I. Ogino and Y. Miyake, *Chem. Lett.*, 1979, 17; K. D. Kreuer, M. Hampele, K. Dolde and A. Rabenau, *Solid State Ionics*, 1988, **28**, 589.
- 30 19 M. Sadakane and E. Stechhan, *Chem. Rev.*, 1998, **98**, 219.
- 20 A. Yokoyama, T. Kojima, K. Ohkubo and S. Fukuzumi, *Chem. Commun.*, 2007, 3997; A. Yokoyama, T. Kojima, K. Ohkubo and S. Fukuzumi, *Inorg. Chem.*, 2010, **49**, 11190.
- 35 21 V. Mahadevan, J. L. DuBois, B. Hedman, K. O. Hodgson and T. D. P. Stack, *J. Am. Chem. Soc.*, 1999, **121**, 5583.
- 22 S.-C. Tsai and J. P. Klinman, *Biochemistry*, 2001, **40**, 2303.
- 23 A. M. Khenkin, I. Efremenko, L. Weiner, J. M. L. Martin and R. Neumann, *Chem.–Eur. J.*, 2010, **16**, 1356.
- 40 24 R. Guillard, K. Perié, J.–M. Barbe, D. J. Nurco, K. M. Smith, E. V. Caemelbecke and K. M. Kadish, *Inorg. Chem.*, 1998, **37**, 973; K. M. Kadish, E. V. Caemelbecke, F. D'Souza, M. Lin, D. J. Nurco, C. J. Medforth, T. P. Forsyth, B. Krattinger, K. M. Smith, S. Fukuzumi, I. Nakanishi and J. A. Shelnut, *Inorg. Chem.*, 1999, **38**, 2188.
- 45 25 Under the catalytic conditions, the formation of benzoic acids from the corresponding aldehydes was observed after 90 min.
- 26 S. Yurdakal, G. Palmisano, V. Loddo, O. Alagöz, V. Augugliaro and L. Leonardo Palmisano, *Green Chem.*, 2009, **11**, 510.
- 27 A. Kumar, P. K. Sharma and K. K. Banerji, *J. Phys. Org. Chem.*, 2002, **15**, 721.
- 50 28 S. Higashimoto, N. Suetsugu, M. Azuma, H. Ohue and Y. Sakata, *J. Catal.*, 2010, **274**, 76.
- 29 Y. Kanda, K. Y. Lee, S. Nakata, S. Asaoka and M. Misono, *Chem. Lett.*, 1988, 139.
- 55 30 K. Y. Lee, N. Mizuno, T. Okuhara and M. Misono, *Bull. Chem. Soc. Jpn.*, 1989, **62**, 1731.
- 31 G. M. Brown, M.–R. Noe-Spirlet, W. R. Bushing and H. A. Levy, *Acta Crystallogr.*, 1977, **B33**, 1038.
- 32 M. Filowitz, W. G. Klemperer, L. Messerle and W. Shum, *J. Am. Chem. Soc.*, 1976, **98**, 2345; W. H. Knoth and R. L. Harlow, *J. Am. Chem. Soc.*, 1981, **103**, 4265; S. Tomomura and A. Aoshima, *Shokubai (Catalyst)*, 1985, **27**, 389.
- 33 For pK_a values of benzyl alcohols in acetonitrile, see: H. Brink, *Acta Pharm. Suec.*, 1980, **17**, 233; Y. Nakagawa, K. Uehara and N. Mizuno, *Inorg. Chem.*, 2005, **44**, 9068.
- 65 34 The EPR signal due to the Ru^{III} center disappeared upon addition of PhIO. This suggests the formation of a $Ru^{IV}=O$ ($S = 1$) species rather than a $Ru^V=O$ ($S = 3/2$ or $1/2$) species.
- 35 K. Ohkubo, Y. Moro-oka and S. Fukuzumi, *Org. Biomol. Chem.*, 2006, **4**, 999; S. Fukuzumi, K. Shimoosako, T. Suenobu, Y. Goto and Y. Watanabe, *J. Am. Chem. Soc.*, 2003, **125**, 9074.
- 70



5 A ruthenium-substituted Keggin-type polyoxometalate forms a molecular assembly with two saddle-distorted Mo^V-porphyrin units to perform catalytic oxidation of benzyl alcohols.